

RESEARCH PAPER

Dextran Grafted Nickel-doped Superparamagnetic Iron Oxide Nanoparticles: Electrochemical Synthesis and Characterization

Mustafa Aghazadeh^{1,*}, Isa Karimzadeh² and Mohammad Reza Ganjali^{3,4}

¹ Materials and Nuclear Research School, Nuclear Science and Technology Research Institute (NSTRI), Tehran, Iran

² Department of Physics, Faculty of Science, Central Tehran Branch, Islamic Azad University, Tehran, Iran

³ Center of Excellence in Electrochemistry, Faculty of Chemistry, University of Tehran, Tehran, Iran

⁴ Biosensor Research Center, Endocrinology and Metabolism Molecular-Cellular Sciences Institute, Tehran University of Medical Sciences, Tehran, Iran

ARTICLE INFO

Article History:

Received 09 February 2019

Accepted 18 March 2019

Published 01 July 2019

Keywords:

Electrochemical Synthesis

Iron Oxide

Magnetic Properties

Nanoparticles

Ni Doping

Surface Capping

ABSTRACT

In this paper, polymer grafted nickel-doped iron oxide nanoparticles are fabricated via an easy, one-step and fast electrochemical procedure. In the deposition experiments, iron(II) chloride hexahydrate, iron(III) nitrate nonahydrate, nickel chloride hexahydrate, and dextran were used as the bath composition. Dextran grafted nickel-doped iron oxides (DEX/Ni-SPIOs) were synthesized with applying direct current (*dc*) of 10 mA cm⁻². The magnetite crystal phase, nano-size, Ni doped content, and dextran grafting onto SPIOs were verified through X-ray powder diffraction (XRD), Fourier transform infrared (FTIR) spectroscopy, field-emission scanning electron microscopy (FE-SEM), transmission electron microscopy (TEM) and thermogravimetric (TG) and differential scanning calorimetry (DSC) analyses. Magnetic evaluation through vibrating-sample magnetometer (VSM) proved that the DEX/Ni-SPIOs product have superparamagnetic behavior with exhibiting the high saturation magnetization and negligible *M_s* and *H_{ci}* values. Based on the obtained results, it was confirmed that the prepared dextran grafted Ni-SPIOs have suitable physico-chemical and magnetic properties for both therapeutic and diagnostic aims.

How to cite this article

NAME N. Dextran Grafted Nickel-doped Superparamagnetic Iron Oxide Nanoparticles: Electrochemical Synthesis and Characterization. *J Nanostruct*, 2019; 9(3): 531-538. DOI: 10.22052/JNS.2019.03.014

INTRODUCTION

Among the various promising candidates for biomedical use, magnetic nanoparticles (MNPs) have received significant attention as a result of their intrinsic magnetic properties. This class of nanomaterials include metallic, bimetallic, and superparamagnetic iron oxides (SPIOs) [1]. For biomedical aims, SPIOs are more interested due to their low toxicity nature and facility of surface engineering with biocompatible agents as well as targeting, imaging, and therapeutic molecules [2]. This flexibility has provided SPIOs to be simply used in magnetic separation, biosensor, in vivo medical imaging, drug delivery, tissue

repair, and hyperthermia applications [3-9]. The magnetic action of SPIOs depends significantly on their shape, size and surface load [10], and these factors are determined by the designed synthesis procedure and applied surface coat onto SPIOs [11]. Hence, various synthesis methods including the coprecipitation, hydrothermal processes, sol-gel, and thermal decomposition have been developed for the synthesise high-quality MNPs [12-17]. In addition to these methods, electrochemical process has been also applied as an easy, non-expensive and fast procedure for preparation of naked and surface coated SPIOs [18-22]. As an electrochemical route, cathodic

* Corresponding Author Email: maghazadeh@aeoi.org.ir

electrodeposition has been introduced as a facile preparation method for the fabrication of nanomaterial due to its ability in controlling crystal phase, size and composition of products [22-27].

As an important factor, surface coating plays essential role in magnetic ability and medical uses of SPIOs. In this regard, it was stressed that although pristine/or uncoated SPIOs are stable in high and low pH mediums, but *in vivo* uses require surface coated SPIOs [28]. For instance, surface capping layer should be able to (a) prevent agglomeration of iron oxide particles, (b) provide chemical bonds for further functionalization of SPIOs with therapeutic and diagnostic agents [29], and enhance their pharmacokinetics, endosomal release, and tailored drug loading and release behaviors [28]. Up now, various polymers including PEG [30], PVA [31], chitosan [32], PEI [33], and PVP [34,35] have been applied as SPIOs surface coat. For applying surface capping onto SPIOs surfaces, several strategies like as covalent linkage, direct nanoparticle conjugation, click chemistry, covalent linker chemistry, and also physical interactions have been employed [36]. It has been found that covalent linkages are strong and stable bonds, which can be specifically formed between functional groups, typically $-NH_2$, $-COOH$, and $-SH$ groups attached onto SPIOs surface and conjugated ligands [36]. Dextran is an abundant, inexpensive polymer that composed of alpha-D-glucopyranosyl monomers, which has a large number of $-OH$ groups to provide covalent linkage and local sites for surface capping of SPIOs, as well as biological compatibility and stability [37]. Hence it is proper candidate for biomedical uses like as hyperthermia and MRI contrast agent [37-39]. Metal cations doping could be also an effective strategy for improving the magnetic properties of SPIOs [40-43]. Recently, we have reported an *in situ* doping of Fe_3O_4 nanoparticles with various metal cations through electrochemical deposition method [44-46], the magnetic evaluations have indicated that the superparamagnetic behavior of iron oxide is improved *via* this strategy [44-46]. Here, we report an electrochemical platform for fabrication of dextran grafted and Ni^{2+} -doped iron oxide nanoparticles (DEX/Ni-SPIOs). The prepared SPIOs are characterized through XRD, FE-SEM, FT-IR, DSC-TGA and VSM analyses.

MATERIALS AND METHODS

Electrochemical synthesis of DEX/Ni-SPIOs

All chemicals were purchased from Sigma-Aldrich company, and used as received. For preparation of electrodeposition bath; First, 0.15g iron(II) chloride hexahydrate, 0.4g iron(III) nitrate nonahydrate, and 0.05g nickel chloride hexahydrate were dissolved in 100cc distilled water, and then 0.1g dextran (as capping agent) was added into this solution and stirred for 20min. The direct current (*dc*) electrodeposition mode was chosen for synthesis of samples. In *dc* deposition, a two-electrode electrochemical set-up was constructed using a stainless-steel cathode centered between two graphite anodes. After assembling the mentioned electrochemical cell, a typical current density of 10 mA cm^{-2} was applied into this system for 20min at RT condition, and a black film was formed on the steel cathode at the end of deposition time. After this step, the deposited film was collected from the steel electrode, and dispersed in 50cc ethanol solution. Then, this solution was centrifuged at 3000 rpm for 10 min to remove the weekly capped dextran onto the iron oxide surfaces and other impurities. In final stage, the dispersed powder was collected from the ethanol solution by magnet. The collected powder was dried in a vacuum oven at 70°C for 2h, and the obtained black powder was named DEX/Ni-SPIOs product.

Sample characterization

The prepared DEX/Ni-SPIOs powder was tested through field-emission scanning electron microscopy (FE-SEM, Mira 3-XMU with accelerating voltage of 100 kV) and energy dispersive diffraction X-ray analysis (EDX) to identify its morphology and elemental composition. Surface morphology of the sample was also observed by TEM (Model Zeiss EM900). The crystal structure of the prepared sample was recorded by X-ray diffraction (XRD, Phillips PW-1800) using a $Co \text{ K}\alpha$ radiation. Thermal behavior of the sample was studied using a thermo-analyzer, model STA-1500. This analysis was done in N_2 atmosphere at the temperatures of 25-600 $^\circ\text{C}$ with applying a heating rate of 5°C min^{-1} . The FTIR spectra were collected in the wavenumber range of 400 to 4000 cm^{-1} using a Bruker Vector 22 Fourier transformed infrared spectroscope. The magnetic curves of the prepared DEX/Ni-SPIOs were provided in the

range of -20000 to 20000 Oe at RT using vibrating sample magnetometer (Meghnatis Daghigh Kavir Co., Iran).

RESULTS AND DISCUSSION

Fig. 1 presets the XRD pattern of dextran grafted Ni-SPIOs. The recorded pattern showed typical iron oxide diffraction peaks, suggesting good crystallinity. The size broadening indicates the nanometer size of the SPIOs crystallites. The observed peaks at 21.23°, 35.18°, 41.44°, 50.75°, 63.05°, 67.36°, and 74.35° are well matched with the (111), (220), (311), (400), (422), (511)

and (440) crystal planes of magnetite. Hence, the prepared sample has been crystallized into the magnetite phase (JCPDS card No. 01-088-0315). By the Debye–Sherrer equation ($D=K\lambda/\beta\cos\theta$), the average crystallite size was obtained to be 8.7nm.

FT-IR test was provided to verify the grafting of the electrosynthesized SPIOs with dextran agent. In fact, this analysis was used to determine the chemical composition of sample and prove the presence of dextran onto the surface of Ni-SPIOs particles. Fig. 2 shows the FT-IR spectrum of the DEX/Ni-SPIOs sample. Generally, the IR peaks observed at the wavenumbers lower that 700cm⁻¹

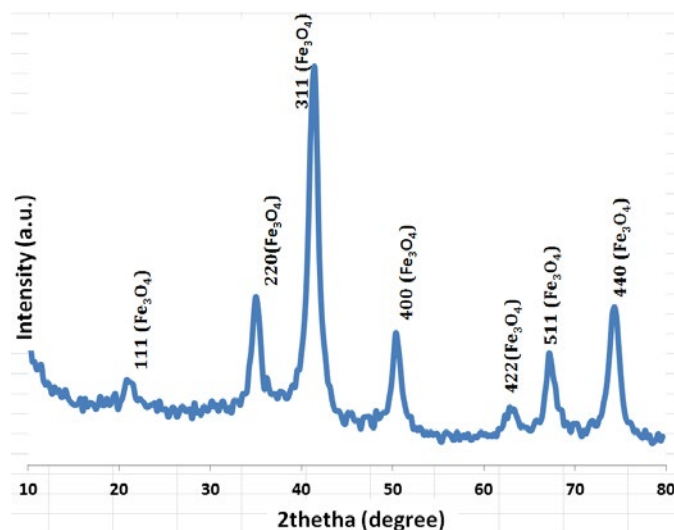


Fig. 1. XRD pattern of the prepared DEX/Ni-SPIOs sample.

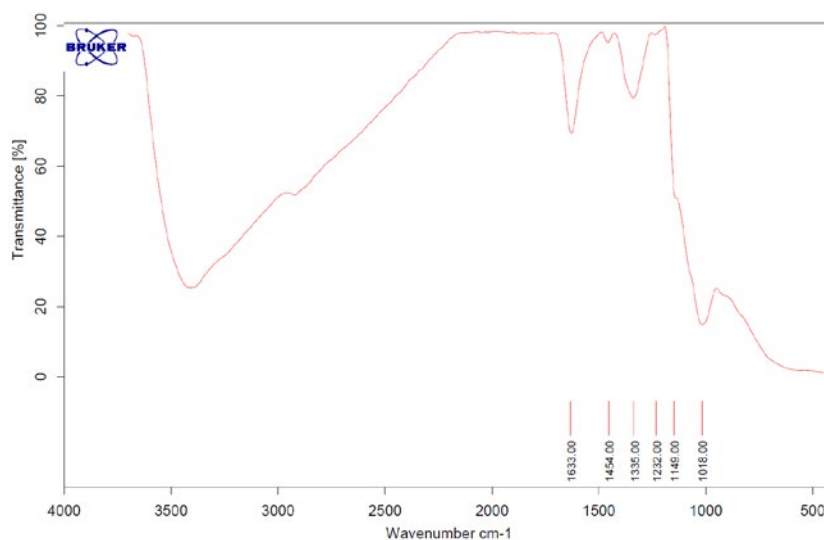


Fig. 2. IR spectrum of the fabricated DEX/Ni-SPIOs sample.

implicate the metal-oxygen vibrations (i.e. $\nu_{(\text{Fe-O-Fe})}$ and $\nu_{(\text{Ni-O-Fe})}$) [47,48]. In this spectrum, the other IR peaks are due to the following vibrations [37,38,47-50]; the band at 1633 cm^{-1} is due to the vibration of water molecules bonded onto Ni-SPIOs particles, the bands at 2927 and 2893 cm^{-1} are resulted from the asymmetric and symmetric vibrations of C-H bonds in dextran, the peak at 1149 cm^{-1} is caused by covalent vibrations of the dextran glycosidic bridge, the peak at 997 cm^{-1} is due to the vibration of the C-O bond at the C-4 position of the glucose residue, and the bands observed at 1454 , 1355 and 1232 cm^{-1} are related to the deformation vibrations of H-C-OH bands in the dextran chains. The presence of these vibrational modes is proved surface grafting of SPIOs by dextran [29]. Hence, these IR data demonstrate that the surfaces of Ni-doped iron oxide nanoparticles are covered with dextran polymer during the electrodeposition synthesis.

The differential scanning calorimetry (DSC) and the related weight loss data were recorded in the temperature range of $25\text{--}600\text{ }^\circ\text{C}$ and the resulted profiles are shown in Fig. 3. In the DSC curve (Fig. 3a), an endothermic peak is occurred in the temperature range of $25\text{--}150\text{ }^\circ\text{C}$, which is due to the evaporation of water molecules attached onto the Ni-SPIOs particles and also OH groups in dextran chain [52-54]. TG curve showed about 2.5% weight reduction for this physical change. After this step, DSC profile exhibited two-successive endothermic peaks between temperatures of 150 to $350\text{ }^\circ\text{C}$. Correspondingly, TG curve has a sharp weight loss

(about 9.3%) at these temperatures (as clearly seen in Fig. 3b). Notably, it was reported that iron oxide NPs coated with dextran show a sharp weight loss at the temperature range of $150\text{--}300\text{ }^\circ\text{C}$, due to the two-step degradation of dextran coat [54-56]. Hence, the changes observed in TG curve at $T=150\text{--}350\text{ }^\circ\text{C}$ are assigned to the breakdown of organic skeleton in dextran. At final step, there is a small endothermic peak and weight loss (0.3%) at temperature of $550\text{ }^\circ\text{C}$, which can be related to the phase transition of Fe_3O_4 into FeO [57]. The total weight loss of DEX Ni-SPIOs was found to be 12.1%. These results clearly approved the dextran grafting onto the synthesized DEX/Ni-SPIOs.

FE-SEM and TEM images and the elemental analysis (i.e. EDAX) profile of DEX/Ni-SPIOs sample are presented in Fig. 4. From FE-SEM observation in Fig. 4a, it is revealed that the sample has been electrodeposited and growth in spherical particles morphology with an average size of 10 nm . TEM observation in Fig. 4c is also revealed that the prepared particles have spherical form with mean size of 10 nm . Furthermore, the EDAX data showed that the DEX/Ni-SPIOs sample has Fe, Ni, O and C elements with weight percentages of 46.42%, 6.07%, 36.51% and 11% in its chemical composition. These data verified that the iron oxides have been doped by Ni (6.07wt%) during electrochemical synthesis. Furthermore, the presence of 11wt% carbon in chemical composition of the deposited sample implicated the surface grafting of the deposited iron oxide particles by dextran. These results clearly proved

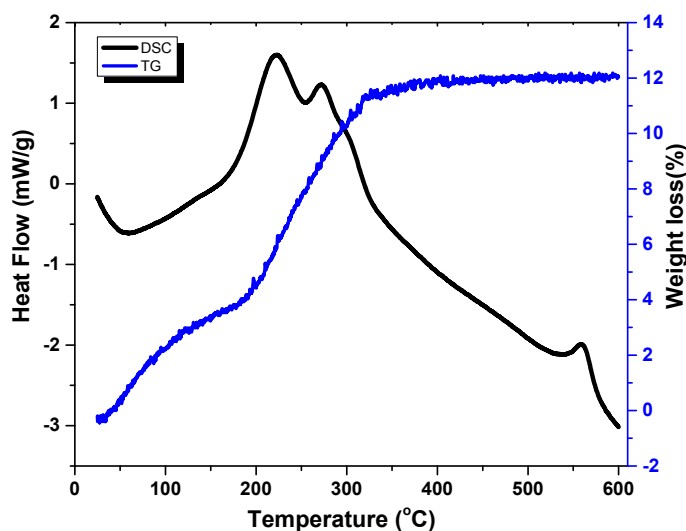


Fig. 3. DSC-TGA curves of the electrodeposited DEX/Ni-SPIOs sample.

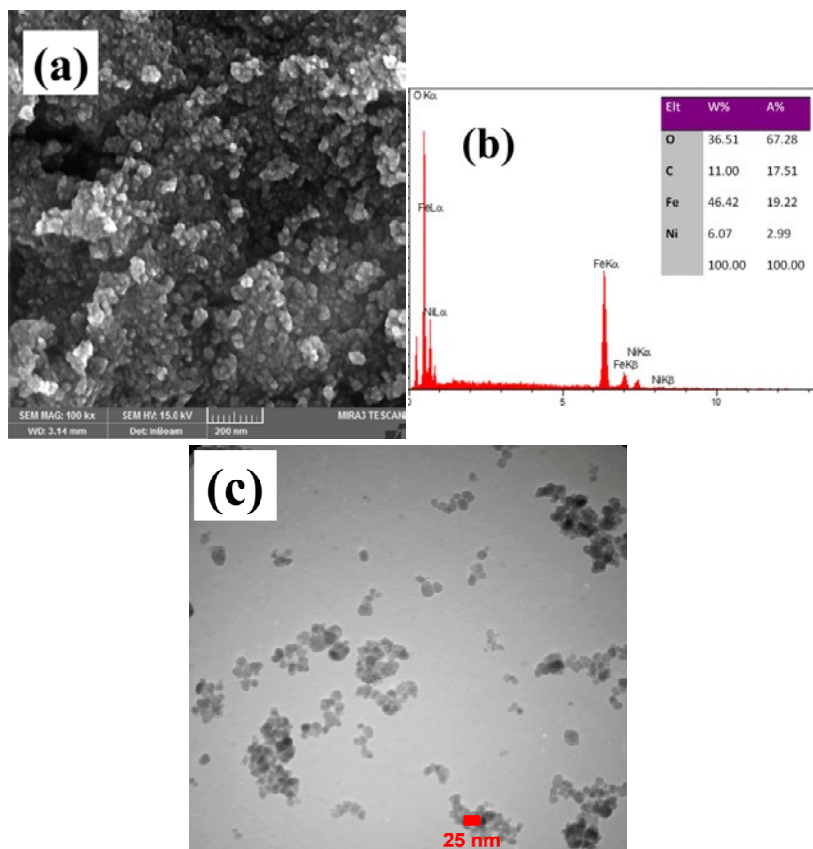


Fig. 4. (a) FE-SEM image, (b) EDAX data and (c) TEM image of the prepared DEX/Ni-SPIOs sample.

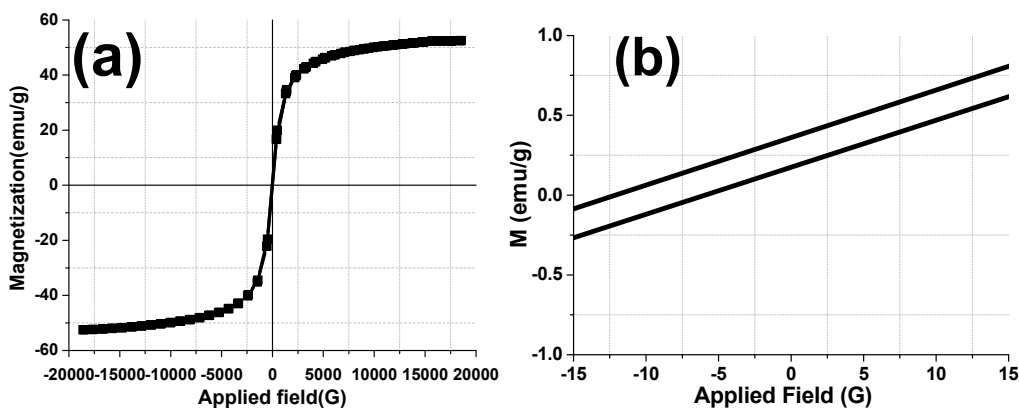


Fig. 5. Hysteresis loops for the electrodeposited the prepared DEX/Ni-SPIOs.

the successful electrosynthesis of surface grafted Ni-doped magnetite nanoparticles.

The magnetic behavior of the fabricated nickel-doped iron oxide particles was measured using vibrating-sample magnetometer (VSM) test. The resulted *M-H* curve is shown in Fig. 5 and also

the related magnetic data are listed in Table 1. The shape of *M-H* profile and also absence of any hysteresis loop implicated the superparamagnetic behavior of our sample [36-38]. As listed in Table 1, the saturation magnetization (*M_s*), remanence (*M_r*) and coercivity (*H_{ci}*) values were

Table 1. Comparison of Magnetic data for naked and coated SPIOs

Sample name	Ms (emu/g)	Mr (emu/g)	Hci (G)	Negative Mr(emu/g)	Positive Mr(emu/g)	Negative Hci (G)	Positive Hci (G)	Refs.
DEX/Ni-SPIOs	52.45	0.13	3.09	0.24	0.51	-12.08	-5.92	This work
Naked SPIOs	72.96	0.95	14.6	2.73	0.83	-12.66	-41.87	46
DEX-SPIOs	15.2	---	---	---	---	---	---	36
DEX-SPIOs	45.87	---	---	---	---	---	---	52
Sm-SPIOs	71.6	12	88.8	---	---	---	---	40
Ni-SPIOs	47.25	0.22	4.34	---	---	---	---	58
Cu-SPIOs	48	5.6	51.8	---	---	---	---	59

found to be 52.45 emu g⁻¹, 0.13 emu g⁻¹ and 3.09 G, respectively. These values revealed that the prepared sample has relative high Ms and negligible Mr and Hci values. As listed in Table 1, it has been reported that the magnetic data for electrochemically synthesized bare iron oxide and bare Ni doped iron oxide have been reported to be: Ms=72.96 emu/g, Mr=0.95 emu/g (for bare SPIOs) [46], and Ms=47.25 emu/g, Mr=0.22 emu/g (for bare Ni-SPIOs) [58]. Furthermore, for dextran coated SPIOs (Ms=15.2 [36], Ms=45.87 [52]), and for metal ion-doped SPIOs (Ms=71.6 emu/g, Mr=12 emu/g and Hci=88.8 G for Sm-SPIOs [40], Ms=47.25 emu/g, Mr=0.22 emu/g and Hci=4.34 G for Ni-SPIOs [58] and Ms=48 emu/g, Mr=5.6 emu/g and Hci=51.8 G for Cu-SPIOs [59] have been reported (Table 1). Comparing these magnetic data with those obtained in this work indicated that the superparamagnetic behavior of iron oxide could be further improved through grafting with dextran polymer as a result of lowering the residual magnetization. After dextran grafting, the DEX/Ni-SPIOs sample exhibited relative high Ms and negligible residual Mr, showing the excellent magnetic performance of these magnetic particles with altering the applied field. This type of magnetic action is very required at various targeting, imaging, and therapeutic applications of SPIOs such as hyperthermia, magnetic therapy and magnetic resonance imaging [3-9]. Hence, it was concluded that the prepared dextran grafted Ni-SPIOs have suitable physico-chemical and magnetic properties for both therapeutic and diagnostic aims.

CONCLUSION

In summary, an easy electrochemical method was constructed for the preparation of dextran grafted nickel-doped iron oxide nanoparticles. The magnetite crystal phase of the deposited powder was proved via XRD and FT-IR data. FE-

SEM and TEM observations revealed the size of prepared particles are 10nm and EDAX data exhibited about 6% Ni doping into SPIOs structure. Thermogravimetric data showed 10%wt surface grafting of Ni-SPIOs by dextran polymer. The obtained VSM results indicated that the fabricated sample has low remnant magnetization and coercivity (i.e. Mr=0.13 emu/g and Hci=3.09 G), establishing its suitability for biomedical applications.

CONFLICT OF INTEREST

The authors declare that there are no conflicts of interest regarding the publication of this manuscript.

REFERENCES

1. Lima-Tenório MK, Gómez Pineda EA, Ahmad NM, Fessi H, Elaissari A. Magnetic nanoparticles: In vivo cancer diagnosis and therapy. *International Journal of Pharmaceutics*. 2015;493(1-2):313-27.
2. Tietze R, Zaloga J, Unterweger H, Lyer S, Friedrich RP, Janko C, et al. Magnetic nanoparticle-based drug delivery for cancer therapy. *Biochemical and Biophysical Research Communications*. 2015;468(3):463-70.
3. Wang Z, Qiao R, Tang N, Lu Z, Wang H, Zhang Z, et al. Active targeting theranostic iron oxide nanoparticles for MRI and magnetic resonance-guided focused ultrasound ablation of lung cancer. *Biomaterials*. 2017;127:25-35.
4. Gonçalves LC, Seabra AB, Pelegrino MT, de Araujo DR, Bernardes JS, Haddad PS. Superparamagnetic iron oxide nanoparticles dispersed in Pluronic F127 hydrogel: potential uses in topical applications. *RSC Advances*. 2017;7(24):14496-503.
5. Singh N, Patel K, Sahoo SK, Kumar R. Human nitric oxide biomarker as potential NO donor in conjunction with superparamagnetic iron oxide @ gold core shell nanoparticles for cancer therapeutics. *Colloids and Surfaces B: Biointerfaces*. 2018;163:246-56.
6. Ta HT, Li Z, Hagemeyer CE, Cowin G, Zhang S, Palasubramaniam J, Alt K, Wang X, Peter K, Whittaker AK. Molecular Imaging of Activated Platelets via Antibody-targeted Ultrasmall Iron Oxide Nanoparticles Displaying Unique Dual MRI Contrast. *Biomater*, 2017; 134: 31-42.
7. Kandasamy G, Sudame A, Maity D. ATA and TA coated superparamagnetic iron oxide nanoparticles: Promising



- candidates for magnetic hyperthermia therapy. *Advanced Materials Letters*. 2017;8(8):873-7.
8. Yang R-M, Fu C, Fang J, Xu X, Wei X, Tang W, et al. Hyaluronan-modified superparamagnetic iron oxide nanoparticles for bimodal breast cancer imaging and photothermal therapy. *International Journal of Nanomedicine*. 2016;Volume 12:197-206.
 9. Zheng J, Ren W, Chen T, Jin Y, Li A, Yan K, et al. Recent Advances in Superparamagnetic Iron Oxide Based Nanoprobes as Multifunctional Theranostic Agents for Breast Cancer Imaging and Therapy. *Current Medicinal Chemistry*. 2018;25(25):3001-16.
 10. Guardia P, Labarta A, Batlle X. Tuning the Size, the Shape, and the Magnetic Properties of Iron Oxide Nanoparticles. *The Journal of Physical Chemistry C*. 2010;115(2):390-6.
 11. Issa B, Obaidat I, Albiss B, Haik Y. Magnetic Nanoparticles: Surface Effects and Properties Related to Biomedicine Applications. *International Journal of Molecular Sciences*. 2013;14(11):21266-305.
 12. Shahrekizad M, Gholamalizadeh Ahangar A, Mir N. EDTA-Coated Fe₃O₄ Nanoparticles: a Novel Biocompatible Fertilizer for Improving Agronomic Traits of Sunflower (*Helianthus Annuus*). *J Nanostruct*, 2015; 5: 117- 127.
 13. Gholami L, Kazemi Oskuee R, Tafaghodi M, Ramezani Farkhani A, Darroudi M. Green facile synthesis of low-toxic superparamagnetic iron oxide nanoparticles (SPIONs) and their cytotoxicity effects toward Neuro2A and HUVEC cell lines. *Ceramics International*. 2018;44(8):9263-8.
 14. Sodipo BK, Aziz AA. One minute synthesis of amino-silane functionalized superparamagnetic iron oxide nanoparticles by sonochemical method. *Ultrasonics Sonochemistry*. 2018;40:837-40.
 15. Belaid S, Stanicki D, Vander Elst L, Muller RN, Laurent S. Influence of experimental parameters on iron oxide nanoparticle properties synthesized by thermal decomposition: size and nuclear magnetic resonance studies. *Nanotechnology*. 2018;29(16):165603.
 16. Kratz H, Taupitz M, Ariza de Schellenberger A, Kosch O, Eberbeck D, Wagner S, Wagner S, Novel magnetic multicore Nanoparticles designed for MPI and other biomedical applications: From synthesis to first in vivo studies. *PLoS ONE*, 2018; 13(1): e0190214.
 17. Heidari A, Mir N, Nikkaran AR. Phenylalanine Removal from Water by Fe₃O₄ Nanoparticles Functionalized with Two Different Surfactants. *J Nanostruct*, 2016; 6(3): 199-206.
 18. Karimzadeh I, Aghazadeh M, Ganjali MR, Norouzi P, Doroudi T, Kolivand PH. Saccharide-coated superparamagnetic Fe₃O₄ nanoparticles (SPIONs) for biomedical applications: An efficient and scalable route for preparation and in situ surface coating through cathodic electrochemical deposition (CED). *Materials Letters*. 2017;189:290-4.
 19. Aghazadeh M, Karimzadeh I, Ganjali MR. Electrochemical evaluation of the performance of cathodically grown ultra-fine magnetite nanoparticles as electrode material for supercapacitor applications. *Journal of Materials Science: Materials in Electronics*. 2017;28(18):13532-9.
 20. Karimzadeh I, Aghazadeh M, Doroudi T, Ganjali M, Kolivand P. Effective Preparation, Characterization and In Situ Surface Coating of Superparamagnetic Fe₃O₄ Nanoparticles with Polyethyleneimine Through Cathodic Electrochemical Deposition (CED). *Current Nanoscience*. 2017;13(2):167-74.
 21. Aghazadeh M, Karimzadeh I, Ganjali MR, Mohebi Morad M. A novel preparation method for surface coated superparamagnetic Fe₃O₄ nanoparticles with vitamin C and sucrose. *Materials Letters*. 2017;196:392-5.
 22. Karimzadeh I, Dizaji HR, Aghazadeh M. Development of a facile and effective electrochemical strategy for preparation of iron oxides (Fe₃O₄ and γ-Fe₂O₃) nanoparticles from aqueous and ethanol mediums and in situ PVC coating of Fe₃O₄ superparamagnetic nanoparticles for biomedical applications. *Journal of Magnetism and Magnetic Materials*. 2016;416:81-8.
 23. Aghazadeh M, Barmi A-AM, Hosseinifard M. Nanoparticulates Zr(OH)₄ and ZrO₂ prepared by low-temperature cathodic electrodeposition. *Materials Letters*. 2012;73:28-31.
 24. Aghazadeh M. Synthesis, characterization, and study of the supercapacitive performance of NiO nanoplates prepared by the cathodic electrochemical deposition-heat treatment (CED-HT) method. *Journal of Materials Science: Materials in Electronics*. 2016;28(3):3108-17.
 25. Aghazadeh M, Ganjali MR. Samarium-doped Fe₃O₄ nanoparticles with improved magnetic and supercapacitive performance: a novel preparation strategy and characterization. *Journal of Materials Science*. 2017;53(1):295-308.
 26. Aghazadeh M, Ghannadi Maragheh M, Ganjali MR, Norouzi P. Preparation and characterization of Mn₅O₈ nanoparticles: A novel and facile pulse cathodic electrodeposition followed by heat treatment. *Inorganic and Nano-Metal Chemistry*. 2017;47(7):1085-9.
 27. Aghazadeh M. One-step cathodic electrosynthesis of surface capped Fe₃O₄ ultra-fine nanoparticles from ethanol medium without using coating agent. *Materials Letters*. 2018;211:225-9.
 28. Kang T, Li F, Baik S, Shao W, Ling D, Hyeon T. Surface design of magnetic nanoparticles for stimuli-responsive cancer imaging and therapy. *Biomaterials*. 2017;136:98-114.
 29. Ali A, Zafar H, Zia M, ul Haq I, Phull AR, Ali JS, et al. Synthesis, characterization, applications, and challenges of iron oxide nanoparticles. *Nanotechnology, Science and Applications*. 2016;Volume 9:49-67.
 30. Karimzadeh I, Dizaji HR, Aghazadeh M. Preparation, characterization and PEGylation of superparamagnetic Fe₃O₄ nanoparticles from ethanol medium via cathodic electrochemical deposition (CED) method. *Materials Research Express*. 2016;3(9):095022.
 31. Sakulkhu U, Mahmoudi M, Maurizi L, Salaklang J, Hofmann H. Protein Corona Composition of Superparamagnetic Iron Oxide Nanoparticles with Various Physico-Chemical Properties and Coatings. *Scientific Reports*. 2014;4(1).
 32. Aghazadeh M, Karimzadeh I. One-pot Electro-synthesis and Characterization of Chitosan Capped Superparamagnetic Iron Oxide Nanoparticles (SPIONs) from Ethanol Media. *Current Nanoscience*. 2017;14(1).
 33. Steitz B, Hofmann H, Kamau SW, Hassa PO, Hottiger MO, von Rechenberg B, et al. Characterization of PEI-coated superparamagnetic iron oxide nanoparticles for transfection: Size distribution, colloidal properties and DNA interaction. *Journal of Magnetism and Magnetic Materials*. 2007;311(1):300-5.
 34. Karimzadeh I, Aghazadeh M, Ganjali MR, Norouzi P, Shirvani-Arani S, Doroudi T, et al. A novel method for preparation of bare and poly(vinylpyrrolidone) coated superparamagnetic iron oxide nanoparticles for biomedical applications.

- Materials Letters. 2016;179:5-8.
35. Aghazadeh M, Karimzadeh I, Ganjali MR. PVP coated Mn²⁺ doped Fe₃O₄ Nanoparticles: A Novel Preparation Method, Surface Engineering and Characterization. Mater Lett, 2018; 228: 137-140.
 36. Peng M, Li H, Luo Z, Kong J, Wan Y, Zheng L, et al. Dextran-coated superparamagnetic nanoparticles as potential cancer drug carriers in vivo. Nanoscale. 2015;7(25):11155-62.
 37. Osborne EA, Atkins TM, Gilbert DA, Kauzlarich SM, Liu K, Louie AY. Rapid microwave-assisted synthesis of dextran-coated iron oxide nanoparticles for magnetic resonance imaging. Nanotechnology. 2012;23(21):215602.
 38. Balas M, Steluta Ciobanu C, Burtea C, Silvia Stan M, Bezirtzoglou E, Predoi D, Dinischiotu A. Synthesis, Characterization, and Toxicity Evaluation of Dextran-Coated Iron Oxide Nanoparticles. Metals, 2017; 7(2): 63-69.
 39. Qin H, Xu D, Yang S. Dextran-coated Fe₃O₄ magnetic nanoparticles as a contrast agent in thermoacoustic tomography for hepatocellular carcinoma detection. Journal of Physics: Conference Series. 2011;277:012028.
 40. Lastovina TA, Budnyk AP, Kudryavtsev EA, Nikolsky AV, Kozakov AT, Chumakov NK, et al. Solvothermal synthesis of Sm³⁺-doped Fe₃O₄ nanoparticles. Materials Science and Engineering: C. 2017;80:110-6.
 41. Aghazadeh M, Karimzadeh I, Ganjali MR, Behzad A. Mn²⁺-doped Fe₃O₄ nanoparticles: a novel preparation method, structural, magnetic and electrochemical characterizations. Journal of Materials Science: Materials in Electronics. 2017;28(23):18121-9.
 42. Aghazadeh M, Ganjali MR. One-pot electrochemical synthesis and assessment of super-capacitive and superparamagnetic performances of Co²⁺ doped Fe₃O₄ ultra-fine particles. Journal of Materials Science: Materials in Electronics. 2017;29(3):2291-300.
 43. Jiang P-S, Tsai H-Y, Drake P, Wang F-N, Chiang C-S. Gadolinium-doped iron oxide nanoparticles induced magnetic field hyperthermia combined with radiotherapy increases tumour response by vascular disruption and improved oxygenation. International Journal of Hyperthermia. 2017:1-9.
 44. Aghazadeh M, Ganjali MR. Evaluation of supercapacitive and magnetic properties of Fe₃O₄ nano-particles electrochemically doped with dysprosium cations: Development of a novel iron-based electrode. Ceramics International. 2018;44(1):520-9.
 45. Aghazadeh M. Zn-doped magnetite nanoparticles: development of novel preparation method and evaluation of magnetic and electrochemical capacitance performances. Journal of Materials Science: Materials in Electronics. 2017;28(24):18755-64.
 46. Aghazadeh M, Karimzadeh I, Ganjali MR, Maragheh MG. Electrochemical fabrication of praseodymium cations doped iron oxide nanoparticles with enhanced charge storage and magnetic capabilities. Journal of Materials Science: Materials in Electronics. 2017;29(6):5163-72.
 47. Zhang JL, Srivastava RS, Misra RDK. Core-Shell Magnetite Nanoparticles Surface Encapsulated with Smart Stimuli-Responsive Polymer: Synthesis, Characterization, and LCST of Viable Drug-Targeting Delivery System. Langmuir. 2007;23(11):6342-51.
 48. Khalkhali M, Sadighian S, Rostamizadeh K, Khoeini F, Naghibi M, Bayat N, et al. Synthesis and characterization of dextran coated magnetite nanoparticles for diagnostics and therapy. BiImpacts. 2017;5(3):141-50.
 49. Karimzadeh I, Aghazadeh M, Doroudi T, Ganjali MR, Kolivand PH, Gharailou D. Superparamagnetic Iron Oxide Nanoparticles Modified with Alanine and Leucine for Biomedical Applications: Development of a Novel Efficient Preparation Method. Current Nanoscience. 2017;13(3):274-80.
 50. Palchoudhury S, Hyder F, Vanderlick TK, Geerts N. Water-Soluble Anisotropic Iron Oxide Nanoparticles: Dextran-Coated Crystalline Nanoplates and Nanoflowers. Particulate Science and Technology. 2014;32(3):224-33.
 51. Predescu AM, Matei E, Berbecaru AC, Pantilimon C, Drăgan C, Vidu R, et al. Synthesis and characterization of dextran-coated iron oxide nanoparticles. Royal Society Open Science. 2018;5(3):171525.
 52. Saraswathy A, Nazeer SS, Nimi N, Arumugam S, Shenoy SJ, Jayasree RS. Synthesis and characterization of dextran stabilized superparamagnetic iron oxide nanoparticles for in vivo MR imaging of liver fibrosis. Carbohydrate Polymers. 2014;101:760-8.
 53. You DG, Saravanakumar G, Son S, Han HS, Heo R, Kim K, et al. Dextran sulfate-coated superparamagnetic iron oxide nanoparticles as a contrast agent for atherosclerosis imaging. Carbohydrate Polymers. 2014;101:1225-33.
 54. Juríková A, Csach K, Miškuf J, Konerácká M, Závěšová V, Kubovčíková M, et al. Thermal Analysis of Magnetic Nanoparticles Modified with Dextran. Acta Physica Polonica A. 2012;121(5-6):1296-8.
 55. Carp O, Patron L, Culita DC, Budrugaec P, Feder M, Diamandescu L. Thermal analysis of two types of dextran-coated magnetite. Journal of Thermal Analysis and Calorimetry. 2009;101(1):181-7.
 56. Hauser AK, Mathias R, Anderson KW, Zach Hilt J. The effects of synthesis method on the physical and chemical properties of dextran coated iron oxide nanoparticles. Materials Chemistry and Physics. 2015;160:177-86.
 57. Khoobi M, Motevalizadeh SF, Asadgol Z, Forooutanfar H, Shafiee A, Faramarzi MA. Polyethyleneimine-modified superparamagnetic Fe₃O₄ nanoparticles for lipase immobilization: Characterization and application. Materials Chemistry and Physics. 2015;149-150:77-86.
 58. Aghazadeh M, Ganjali MR. One-step electro-synthesis of Ni²⁺ doped magnetite nanoparticles and study of their supercapacitive and superparamagnetic behaviors. Journal of Materials Science: Materials in Electronics. 2017;29(6):4981-91.
 59. Huang X, Xu C, Ma J, Chen F. Ionothermal synthesis of Cu-doped Fe₃O₄ magnetic nanoparticles with enhanced peroxidase-like activity for organic wastewater treatment. Advanced Powder Technology. 2018;29(3):796-803.